Calculation of Transient Torques on Motors During a Residual Voltage Motor Bus Transfer

Murty V.V.S. Yalla, *Fellow, IEEE*, Arman Vakili, *Senior Member, IEEE*, and Thomas R. Beckwith, *Life Member, IEEE*

***Abstract*—To maintain a critical process upon loss of primary motor bus power, the petrochemical industry depends largely on residual voltage transfer, ignoring phase angle and closing the backup source when the motor bus residual voltage has decayed to 30%. To assess the consequences of out-of-phase residual voltage transfers, a transient simulation program models a bus with three motors of various sizes, inertias, and impedances. The three motors are loaded around 80% with fan, pump, and compressor loads to calculate the peak transient motor current and torque upon closure of the backup source breaker. Pre-transfer events and conditions produce an initial phase angle between the primary and backup sources, and the simulation reproduces the resultant residual voltage transfer closing angle and its effect on the peak transient current and torque. Individual motors exhibit positive and negative torques, oscillating from induction generator to motor, and the peak-to-peak torques are also recorded, as they can impact the motor shaft stress.**

***Index Terms*—Fast transfer, in-phase transfer, main-tie-main, motor bus transfer (MBT), residual voltage transfer.**

I. Introduction

IN CRITICAL industrial process applications where electric motors are used, any loss of electrical power source can shut down the plant process, causing millions of dollars in losses. Generally in these applications, a backup source of power is provided and the motor busses are transferred from the primary source to the backup source in order to keep the process running without any interruption. ANSI/NEMA Standard C50.41-2012, Polyphase Induction Motors for Power Generating Stations states "Induction motors are inherently capable of developing transient current and torque considerably in excess of rated current and torque when exposed to out-of-phase bus transfer or momentary voltage interruptions and reclosing on the same bus. The magnitude of this transient current and torque may range from 2 to 20 times rated … subjects the motor (including the motor windings) and driven equipment to transient forces in excess of normal running values. Accordingly, each bus transfer or reclosing reduces the life expectancy of the motor by some finite value…" [1]. Industry standards define motor bus transfer (MBT) synchronous methods, which will limit the amount of transient current and torques to safe limits. IEEE Std. C37.96-2012 IEEE Guide for AC Motor Protection defines in-phase transfer as "An open-transition method wherein the close command to the new breaker occurs at a phase angle in advance of phase coincidence between the motor bus and the new source to compensate for the new breaker's closing time" [2].

However, the majority of the MBT applications presently in use today are based on a technique called residual voltage transfer which IEEE Std. C37.96 defines as "An open-transition method wherein the voltage magnitude at the motor bus falls below a predetermined level before the close command is issued to the new breaker. There is no supervision of the synchronous condition between the motor bus and the new source" [3]. ANSI/NEMA C50.41 encourages this method, stating that "A slow transfer or reclosing is defined as one in which the length of time between disconnect of the motor from the power supply and reclosing onto the same or another power supply is delayed until the motor rotor flux linkages have decayed sufficiently so that the transient current and torque associated with the bus transfer or reclosing will remain within acceptable levels…" [1]. It further states that this "can be accomplished by a time delay relay equal to or greater than 1.5 times the open-circuit alternating-current time constant of the motor" [1]. This is the time for the self-generated voltage to decay to 22.3% of rated bus voltage or 26.8 Vac on a 120 Vac VT secondary. ANSI/NEMA C50.41 adds that to "limit the possibility of damaging the motor or driven equipment, or both, it is recommended that the system be designed so that the resultant volts per hertz vector between the motor residual volts per hertz vector and the incoming source volts per hertz vector at the instant the transfer or reclosing is completed does not exceed 1.33 per unit volts per hertz on the motor rated voltage and frequency bases" [1].

The purpose of this article is to study the individual peak transient motor current and torque immediately following the closure of the alternate source breaker using the residual voltage transfer method. A commercially available transient simulation program is used in this article to model three motors of various sizes, inertia, impedance, and loads to calculate the peak transient motor current and torque. Individual motors exhibit

Manuscript received April 15, 2018; revised June 29, 2020; accepted July 9, 2020. Date of publication August 11, 2020; date of current version November 19, 2020. Paper 2018-PCIC-0402.R1, presented at the 2018 Petroleum & Chemical Industry Conference, Cincinnati, OH, USA, Sep. 24–26, 2018, and approved for publication in the IEEE Transactions on Industry Applications by the Petroleum and Chemical Industry Committee of the IEEE Industry Applications Society. *(Corresponding author: Murty V.V.S. Yalla.)*

Murty V.V.S. Yalla and Thomas R. Beckwith are with Beckwith Electric Company, Largo, FL 33773 USA (e-mail: MYalla@BeckwithElectric.com; TBeckwith@BeckwithElectric.com).

Arman Vakili is with Malayer Engineering Services, Perth, WA 6000, Australia (e-mail: Arman.Vakili@mengs.com.au).

Color versions of one or more of the figures in this article are available online at https://ieeexplore.ieee.org.

Digital Object Identifier 10.1109/TIA.2020.3015822

positive and negative transient torques, oscillating from induction generator to motor, and the peak-to-peak torques are also recorded, as they will impact the motor windings, bearings, couplings, gear box, and shaft torsion. The effect of different breaker closing phase angles on the peak transient current and torque are studied by varying the initial phase angle difference between the backup source and primary source. The initial phase angle is varied to achieve different resultant closing phase angles after the residual voltage limit setting has initiated the alternate breaker close command. The transient peak motor current and torque are calculated and reported in per unit (pu) with nominal motor current and nominal torque as base quantities. The study will assess the consequences of out-of-phase residual voltage transfers. Conclusions will be drawn as to the severity of the resultant individual motor torques and currents that will allow a determination if levels have been exceeded that could cause cumulative damage and loss of life to motor windings, bearings, couplings, shafts, loads, source transformers, and cabling. Based on the levels of torques measured, the efficacy of the closing criteria found in ANSI/NEMA C50.41 will be brought into question.

II. Dynamic Conditions Prior to and During Bus Transfer

The justification for the selection of initial phase angles to achieve different resultant closing phase angles is found in IEEE Std. C37.96. Of particular note, and not really acknowledged by some in the industry, are the phenomena described in IEEE Std. C37.96 clause "6.4.8 Events that occur or conditions that exist immediately prior to opening the initial source breaker" [4], and clause 6.4.13 on the transient effects upon disconnection of motor loads immediately after opening this breaker, but prior to the closure of the alternate breaker [5]. This throws out industry paradigms that allow an immediate simultaneous transfer or require a fast transfer be completed within a certain number of cycles. Both assume that the initial phase angle between the motor bus and the new source started somewhere near zero and would thus complete the transfer before the angle has a chance to increase to a damaging level. However, under these phenomena, the initial phase angle between the motor bus and the new source may be nowhere near zero. ANSI/NEMA C50.41 acknowledges the effects of these phenomena in clause 14.3 stating, "test conditions should account for any phase angle difference between the incoming and running power supplies" [6]. The IEEE Std. C37.96 Dynamic Conditions During Bus Transfer are defined as follows [7].

A. *Events That Occur or Conditions That Exist Immediately Prior to Opening the Initial Source Breaker*

1) Faults on the Initial Source

"…will effect a dynamic change in the phase angle just prior to transfer. It is important that dynamic phase angle changes be recognized by the MBT system."

2) Condition of the Alternative Source

"…determine that the events that triggered the transfer (such as a fault on the initial source) have not also affected the alternate source to the point where it is unsuitable to transfer and continue to supply the motor bus."

3) Out-of-Step (OOS) Generator Trip

"The 78 relay is typically programmed to trip when the generator's internal EMF phase is between 120° to 240° relative to the power system. This large internal power angle causes the phase angle across the startup breaker to move to higher than expected values … the motor bus voltage will jump quickly to a new phase angle due to the out-of-step angle of the generator internal voltage."

4) System Separation between Incoming Supply Sources
   a) Different supply voltages can "result in a substantial voltage phase angle difference between the two sources" if "load flow characteristics" vary between two supply systems or if the "systems become separated." Abnormal system operation "can cause a large standing angle between the two sources to the motor bus" due to the "loss of an autotransformer that ties the systems together" or to the "opening of breakers at a ring bus or breaker-and-a-half substation."
   b) Loading of the supply transformers and the "reactive losses that result will cause a voltage phase angle shift between the two sources."

5) Supply Source Transformer Winding Phase Shift

"… there could be an inherent phase shift (30°), between the main and alternate source based on the transformer configuration of the two sources."

B. *Transient Effects Upon Disconnect of Motor Loads*

"… the characteristic of induction motors whereby they exhibit an essentially instantaneous phase shift upon disconnect of motor… This effect is additive to conditions occurring due to other causes…"

But fortunately, given all of these phenomena, an open-transition transfer, which disconnects the motors prior to closing the alternate source, allows the motors to spin free and rotate back through synchronism where the alternate source breaker can always successfully be closed by the synchronous in-phase transfer method. On the contrary, the residual voltage transfer method simply sends a breaker close command when the motor bus voltage drops to 0.3 pu, ignoring the phase angle between the motor bus and the alternate source, so the closing angle could occur anywhere from zero to $+/-180$ degrees.

III. Motor Model Description

A. *Induction Motor Model*

The induction motor model used in this article uses a stationary reference frame for the stator variables and a synchronously rotating reference frame for the rotor variables. The voltages and currents from the simulation are transformed from instantaneous values in the *abc* system to *dq* frame using the Clarke transformation. The *dq* equivalent circuits are given in Fig. 1(a) and (b). The stator core losses are ignored here to simplify the circuit representation.

In Fig. 1, the following variables and parameters are used:

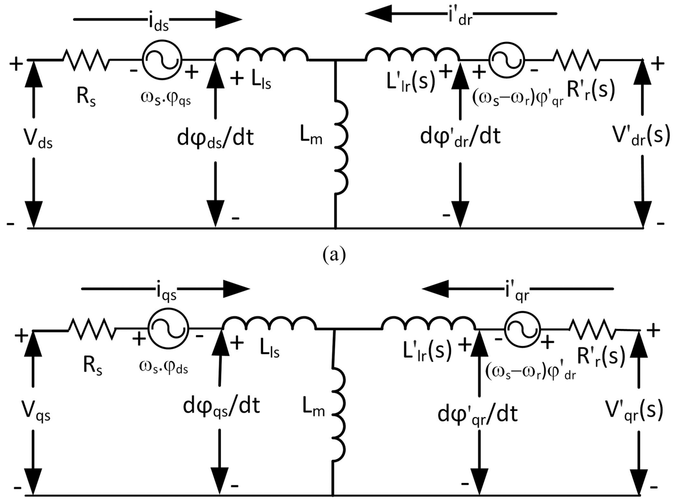

Fig. 1. *dq* model equivalent circuits of an induction motor. (a) *d*-axis and (b) *q*-axis.

V: voltage; I: current; R: Resistance; L: inductance; φ: flux linkages; ω_s: synchronous speed; ω_r: rotor speed; (s): parameter dependent on slip.

The following notation is used for various subscripts:

d: direct axis; *q*: quadrature axis; *s*: stator; *r*: rotor; *m*: mutual.

The flux linkages are given by the following equations:

$$\varphi_{\rm qs} = L_{\rm s} i_{\rm qs} + L_{\rm m} i'_{\rm qr};\ \varphi_{\rm ds} = L_{\rm s} i_{\rm ds} + L_{\rm m} i'_{\rm dr} \tag{1}$$

$$\varphi'_{\rm qr} = L'_{\rm r} i'_{\rm qr} + L_{\rm m} i_{\rm qs};\ \varphi'_{\rm dr} = L'_{\rm r} i'_{\rm dr} + L_{\rm m} i_{\rm ds} \tag{2}$$

$$L_{\rm s} = L_{\rm ls} + L_{\rm m}; L'_{\rm r} = L'_{\rm lr} + L_{\rm m}. \tag{3}$$

The voltages are given by:

$$V_{\rm qs} = R_{\rm s} i_{\rm qs} + d\varphi_{\rm qs}/dt + \omega_s \varphi_{\rm ds} \tag{4}$$

$$V_{\rm ds} = R_{\rm s} i_{\rm ds} + d\varphi_{\rm ds}/dt - \omega_s \varphi_{\rm qs} \tag{5}$$

$$V'_{\rm qr} = R'_{\rm r} i'_{\rm qr} + d\varphi'_{\rm qr}/dt + (\omega_s - \omega_{\rm r})\,\varphi'_{\rm dr} \tag{6}$$

$$V'_{\rm dr} = R'_{\rm r} i'_{\rm dr} + d\varphi'_{\rm dr}/dt - (\omega_s - \omega_{\rm r})\,\varphi'_{\rm qr}. \tag{7}$$

The electromagnetic torque (T_e) is given by:

$$\frac{3}{2} p\,(\varphi_{\rm ds} i_{\rm qs} - \varphi_{\rm qs} i_{\rm ds}) \text{ or } \frac{3}{2} p\,(\varphi_{\rm qr} i'_{\rm dr} - \varphi_{\rm dr} i'_{\rm qr}) \text{ or } \frac{3}{2} p L_{\rm m}\,(i_{\rm qs} i'_{\rm dr} - i_{\rm ds} i'_{\rm qr}) \tag{8}$$

where p is the number of pole pairs.

B. Slip Dependency

The magnitude and frequency of the voltage induced in the rotor at any speed between the extremes of locked rotor (100% slip) and synchronous speed (0% slip) are proportional to the slip of the rotor. The ratio of rotor voltage to rotor current, identified as V'_r and I'_r respectively, in Fig. 2, gives rotor impedance, which changes with slip. The dependency of rotor impedance to rotor speed is not a linear relation. The best way to demonstrate this dependency is to use tabular form as shown in Fig. 3 [8].

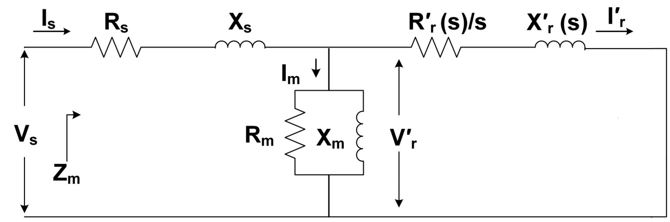

Fig. 2. Electrical circuit representation of an induction motor.

C. Rotor Parameter Calculation

For the purpose of calculating rotor parameters with slip dependency, the following induction motor circuit representation shown in Fig. 2 is used.

Induction motor impedances can be calculated and extracted from the torque-speed curve, power factor speed curve and motor efficiency curve:

$$p_{\rm mech} = \tau \cdot \omega_r \tag{9}$$

$$p_{\rm elect} = I'_r \cdot V'_r \cdot \cos\theta_r = I'^2_r \cdot R'_r(s) \tag{10}$$

where θ_r is the angle between rotor voltage and rotor current.

$$I_m = V'_r \,/\, (R_m + j \cdot X_m) \tag{11}$$

$$V'_r = I'_r \cdot (R_r{}'(s) + j \cdot X'_r(s)) \tag{12}$$

$$I'_r = I_s - I_m \tag{13}$$

$$p_{\rm mech} = \eta \cdot p_{\rm elect}, \text{ where } \eta \text{ is the motor efficiency} \tag{14}$$

$$\omega_r = (1 - s) \cdot \omega_s \tag{15}$$

$$Z_m = [(R'_r(s) + jX'_r(s)) \parallel (R_m + j\,X_m)] + (R_s + j\,X_s). \tag{16}$$

$$\text{The shaft torque, } \tau = \frac{\eta \cdot R'_r(s) \cdot I_s^2}{(1-s) \cdot \omega_s \cdot \left[1 + \frac{R'_r(s) + jX'_r(s)}{R_m + j\,X_m}\right]^2} \tag{17}$$

$$I_s = \frac{V_s}{[(R'_r(s) + jX'_r(s)) \parallel (R_m + j\,X_m)] + (R_s + j\,X_s)} \tag{18}$$

$$P.F. = \cos(\angle V_s - \angle I_s). \tag{19}$$

It is not possible to determine all motor parameters with (17)–(19). Using numerical approximation is the best approach. In this article, a numerical software has been used to calculate the induction motor parameters. An example of this modeling is shown in Fig. 3 [9].

D. MBT One-Line Diagram Model

The model of a simple industrial power system consists of two independent power sources, Main 1 (primary) and Main 2

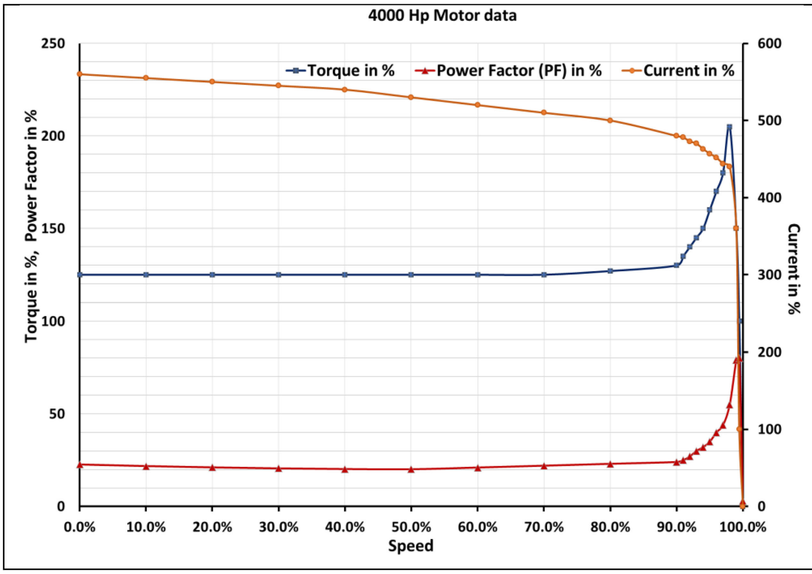

Circuit parameters (refer to Fig. 2)

R_s = 0.66%
X_s = 15.06%
R_m = 4043%
X_m = 383%
R_r (lr) = 3.4%
X_r (lr) = 2.23%
R_r(fl) = 0.56%
X_r(fl) = 11.92%

Calculated slip dependency parameters

Slip (%)	R_r (%)	X_r (%)
100.00	3.40	2.23
90.00	3.38	3.06
80.00	3.33	3.94
70.00	3.20	4.77
60.00	2.91	5.59
50.00	2.50	6.41
40.00	2.15	7.22
30.00	1.79	8.37
20.00	1.43	9.87
10.00	0.86	10.94
9.00	0.86	11.46
8.00	0.86	11.98
7.00	0.86	12.41
6.00	0.84	12.53
5.00	0.79	12.29
4.00	0.74	11.95
3.00	0.69	11.61
2.00	0.60	11.42
1.00	0.57	11.76
0.56	0.56	11.92
0.00	0.54	12.10

Fig. 3. Motor parameter estimation modeling.

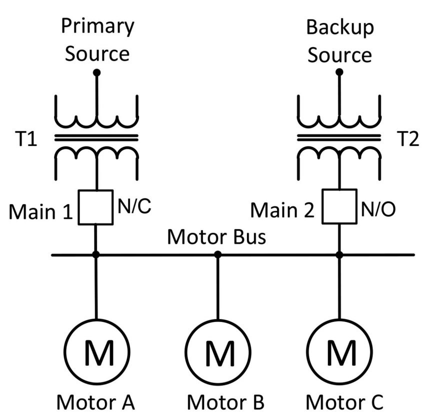

Fig. 4. MBT one-line diagram model.

(backup), and three motors (A, B and C) of different sizes and loads. Fig. 4 shows the one-line diagram of the power system.

E. Motor Model Characteristics

Each motor is modeled based on available motor data, as three motors with different sizes and loads have been chosen to represent an example of an industrial power system. Motor A is a 4000 hp, 4-pole machine, at 4 kV, loaded to 76.9% of full load, connected to a 2500 kW compressor. Motor B is a 1500 hp, 2-pole machine, at 4 kV, loaded to 85.2% of full load, connected to a 1000 kW induced draft fan. Motor C is a 500 hp, 6-pole machine, at 4 kV, loaded to 78.8% of full load, connected to a 300 kW pump. The motor bus is supplied via 13.8/4.16 kV (20 MVA, Z = 5%) transformers T1 and T2.

In order to simulate the realistic condition, the motors are running on primary source (Main 1) at normal condition, and at transfer initiate ($t = 0.1$ s), the primary source is disconnected from the motor bus. The system is equipped with residual voltage transfer scheme to initiate closing of backup source (Main 2) breaker when the motor bus voltage drops to 0.3 pu voltage.

IV. Test and Measurement Methodology

A. Initial Angles Chosen to Produce Different Closing Angles

In this article, the initial angle (voltage angle of Main 2 with respect to Main 1) at time of Main 1 breaker opening, is varied in 30-degree steps in order to simulate a real system with residual voltage transfer closing at various angles. In every case, the peak positive, peak negative, and transient peak-to-peak torques have been measured. The motor bus voltage decays after the separation of source #1 based on the combination of open circuit voltage time constant of the three motors. Each of the three motors can be in generation mode or motor mode depending upon inertia of the motors. A negative torque indicates generation mode and a positive torque indicates motor mode.

B. Transient Peak-to-Peak Torque

The transient peak-to-peak torque is defined as the difference between the positive peak and the negative peak torque the motor experiences (shown in Fig. 5) during various operating conditions such as motor starting, short circuit, and the MBT. The electromagnetic torque can be positive (motor mode) or negative (generator mode). When the motor changes from generator mode to motor mode during the transfer, the reversal of the torque from negative to positive can result in very high transient peak-to-peak torque. This can create stress and fatigue on the shaft and the couplings causing mechanical damage. This is the reason the transient peak-to-peak torque is also reported in this article along with peak positive and peak negative torques.

C. Method to Determine Closing Angle

During the MBT, the motor bus frequency drops from nominal frequency; however, the backup source (Main 2) frequency

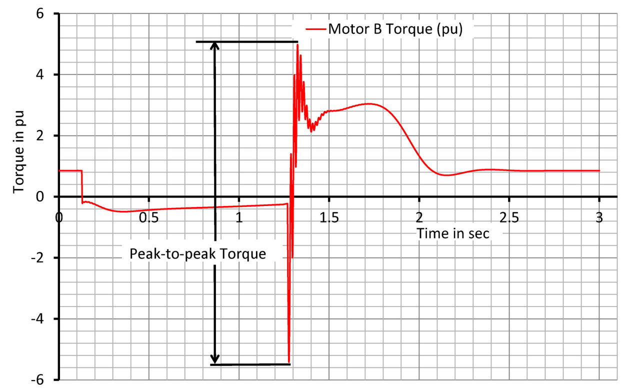

Fig. 5. Transient peak-to-peak torque.

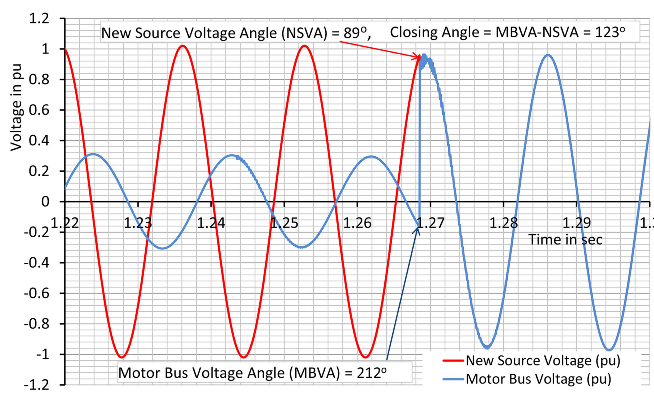

Fig. 6. Closing angle calculation.

remains the same. This difference between the two frequencies (slip frequency) will cause the phase angle between the motor bus and the backup source to change continuously. In this article, the closing angle is calculated based on angular difference between these two waveforms at the moment of closing. The phase angle between the motor bus and the new source is measured from the closest positive-going zero crossings respectively. One full cycle of the respective waveforms prior to closing is considered as 360° for each of the waveforms. The concept is shown in Fig. 6, closing angle calculation.

V. Simulation Tests Performed and Results

Before proceeding with the residual voltage transfer simulation tests, the currents and torques resulting from three other cases are simulated for purposes of comparison with the residual voltage transfer results.

A. Short Circuit Torque During Three-Phase Short Circuit on Motor Terminals

During normal operation, a motor converts electrical energy into mechanical energy. During a short circuit condition, the system voltage will decay. A stable voltage supply no longer exists. The rotating magnetic field in the rotor will attempt to support the reduced voltage condition by becoming a power source. The motor is now providing additional current into the faulted electrical system. This phenomenon is called "motor fault contribution."

Severe short circuit torque (SCT) is produced within a running motor when a fault occurs on the motor circuit. The energy stored in the motor's magnetic field causes it to act briefly as an induction generator, feeding high current to the fault, accompanied by a high transient torque. If that torque is great enough, it can overstress the attachment of the motor to its foundation or damage shafts and couplings in the drive train. Based on industry practice, a typical value of maximum SCT at the shaft or motor base is six times rated torque.

B. Motor Starting From Stopped Condition

An induction motor experiences high stator current and torque during motor starting. Motors are designed to sustain this condition for short periods of time. In this example, the motor starting parameters (lock rotor current and breakdown torque) are also reported in order to compare the transient currents and torques during the bus transfer.

C. In-Phase Transfer (After 10 Cycles)

Pursuant to ANSI/NEMA C50.41 [6], the fast bus transfer can happen only during the first 10 cycles of losing the power supply. However, it is not always possible to perform the transfer during this short window due to a possible large initial phase angle difference between the backup source and the motor bus voltage. Usually after 10 cycles, the motor bus frequency drops considerably to generate a fast rotating phase angle difference between the motor bus and the new source. In such a condition, the circuit breaker (CB) closing time must be taken into account while issuing a close command to achieve CB closing at zero phase angle difference. This bus transfer can happen even after 10 cycles and can transfer the motor bus smoothly. Fig. 7 shows such an in-phase transfer.

D. Residual Voltage Transfer

The residual voltage transfer is performed when the decaying voltage on the bus reaches 0.3 pu without any consideration with respect to phase angle. The method described in Section IV-A. is used to simulate various closing angles for the residual voltage transfer. An example of the waveforms for the residual voltage transfer is shown in Fig. 8. The peak current, transient peak-to-peak torque, positive and negative peak transient torques for various closing angles are shown in Table I and Figs. 9–11.

VI. Discussion and Conclusion From Simulation Results

A. Discussion of Residual Voltage Transfer Results

When the primary source of power is disconnected from the motor bus, the motors start decelerating, and as a result, the bus voltage and frequency gradually decays. In the simulation example, during the deceleration period before closing the backup source of power, the Motor B (1500 hp fan) acts like an induction

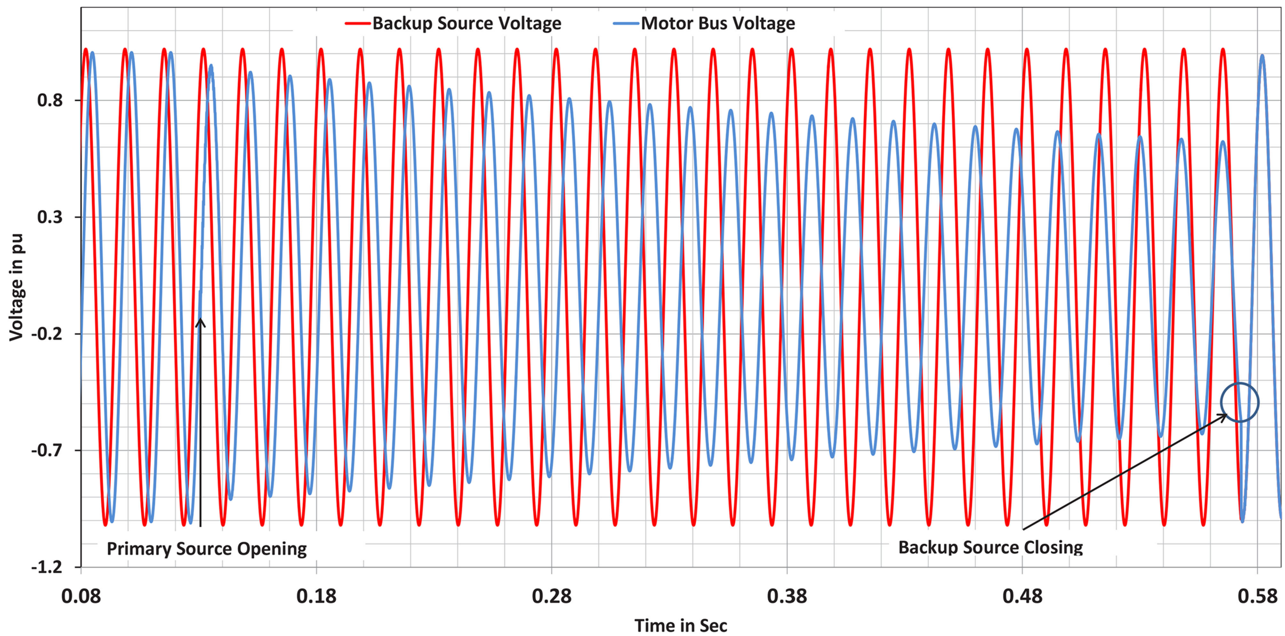

Fig. 7. Voltage waveforms during an in-phase transfer.

TABLE I
RESIDUAL VOLTAGE TRANSFER VERSUS MOTOR START AND IN-PHASE TRANSFER

Closing Angle	25.47	55.47	85.47	115.47	145.47	175.48	205.47	235.47	265.47	295.47	325.47	355.45	**Normal Start**	**In-Phase Transfer**
Motor A Peak Current	**5.36**	**5.46**	**6.44**	**7.44**	**8.54**	**8.59**	**9.05**	**8.69**	**7.63**	**6.90**	**5.55**	**5.22**	**4.70**	**3.44**
Motor B Peak Current	**7.60**	**8.98**	**10.68**	**12.28**	**13.73**	**13.49**	**13.98**	**13.07**	**11.26**	**9.94**	**7.96**	**7.05**	**6.28**	**4.54**
Motor C Peak Current	**6.28**	**6.81**	**8.02**	**9.27**	**10.62**	**10.74**	**11.44**	**11.05**	**9.88**	**9.00**	**7.37**	**6.39**	**5.85**	**3.88**
Motor A Negative Peak Torque	-0.87	-2.06	-3.09	-3.65	-3.56	-2.88	-1.88	-0.88	-0.17	0.00	0.00	0.00	0.00	0.00
Motor B Negative Peak Torque	-2.43	-4.04	-5.17	-5.43	-4.74	-3.40	-1.93	-0.78	-0.49	-0.49	-0.49	-0.94	0.00	-0.49
Motor C Negative Peak Torque	-0.53	-2.09	-3.60	-4.57	-4.74	-4.06	-2.80	-1.41	-0.33	-0.10	-0.10	-0.10	0.00	-0.10
Motor A Positive Peak Torque	3.08	3.27	3.42	3.48	3.28	2.82	2.51	2.06	1.79	2.27	2.47	2.72	1.80	2.95
Motor B Positive Peak Torque	4.66	4.94	5.03	4.87	4.54	4.26	3.87	3.51	3.30	3.76	4.22	4.47	3.24	4.04
Motor C Positive Peak Torque	3.55	3.82	3.85	3.76	3.65	3.32	2.82	2.51	2.29	2.57	2.80	3.14	2.25	3.36
Motor A Transient Pk-to-Pk Torque	**3.95**	**5.33**	**6.52**	**7.13**	**6.83**	**5.70**	**4.39**	**2.94**	**1.97**	**2.27**	**2.47**	**2.72**	**1.80**	**2.95**
Motor B Transient Pk-to-Pk Torque	**7.09**	**8.98**	**10.20**	**10.30**	**9.28**	**7.66**	**5.80**	**4.29**	**3.79**	**4.25**	**4.71**	**5.41**	**3.24**	**4.53**
Motor C Transient Pk-to-Pk Torque	**4.08**	**5.91**	**7.45**	**8.34**	**8.39**	**7.38**	**5.62**	**3.93**	**2.61**	**2.67**	**2.90**	**3.24**	**2.25**	**3.46**
Resultant pu V/Hz	**0.71**	**0.85**	**1.03**	**1.19**	**1.29**	**1.33**	**1.31**	**1.22**	**1.08**	**0.91**	**0.75**	**0.66**		**0.345**

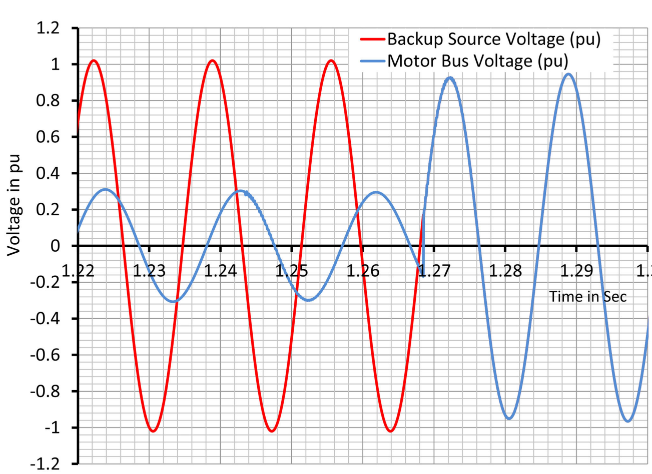

Fig. 8. Voltage waveforms during a residual voltage transfer.

generator (indicated by the negative torque) due to a large inertia of its fan load, supplying electrical power to Motor A (4000 hp compressor) and Motor C (500 hp pump). Even though the bus voltage and frequency are the same on all three motors, the speed and resultant slip are quite different. Referring to Table I, the peak current, peak positive torque, peak negative torque, and peak-to-peak torque occur at different closing angles and the corresponding pu V/Hz.

The peak inrush current on all three motors occurs at a closing angle of 205.47° (pu V/Hz of 1.31) while the peak positive, negative, and transient peak-to-peak torques occur at closing angles in the range of 85.47°–145.47° (pu V/Hz in the range of 1.03–1.29). Considering any peak-to-peak torque above twice the breakdown torque for each motor, we arrive at the following analysis from Table I. The peak-to-peak torque stayed above 4.1 pu (twice the breakdown torque of Motor A) for 50% of the

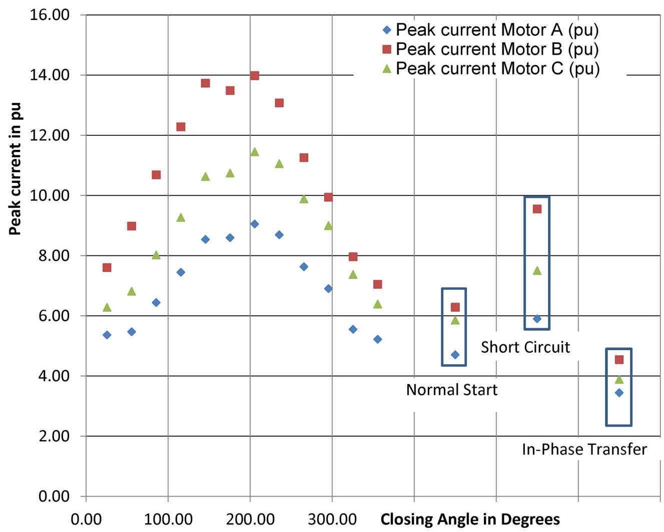

Fig. 9. Graph of peak current versus closing angle.

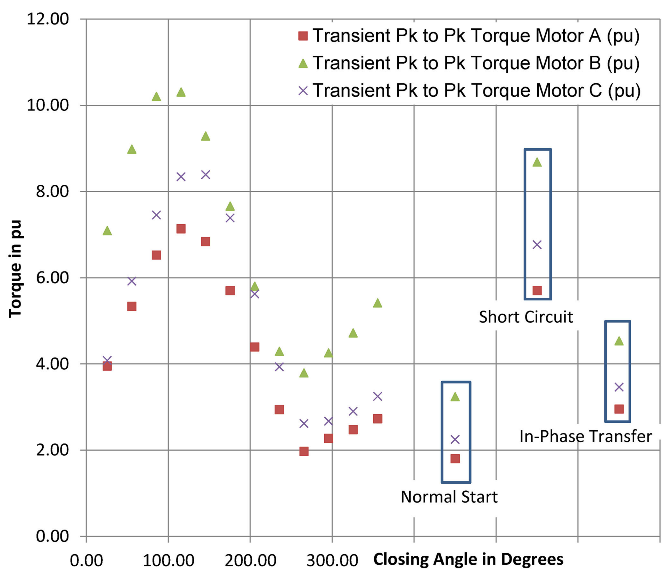

Fig. 10. Graph of transient peak-to-peak torque versus closing angle.

cases for Motor A, stayed above 6.6 (twice the breakdown torque of Motor B) for 50% of the cases for Motor B, and 5.5 (twice the breakdown torque of Motor C) for 50% of the cases for Motor C. Hence, using the ANSI/NEMA C50.41 pu V/Hz limit of 1.33 as a measure to determine if the transient torques and currents exceed the design limits is not of much use as very high inrush currents and torques can occur at V/Hz levels ranging from 0.71 to 1.33 pu.

Reporting the transient peak-to-peak torques, in addition to peak positive and peak negative torques, is important due to the cyclic nature of the shaft torque. The actual cyclic shaft torque can be larger than the electromagnetic torque (the worst-case peak-to-peak electromagnetic torque of 10.30 pu occurs on Motor B at a closing angle of 115.47°) causing mechanical damage depending upon when the motors are reconnected and the magnitude and polarity of the electromagnetic torque immediately after reconnection. The shaft torque when the motor is disconnected can be additive or subtractive to the electromagnetic torque developed after motor reconnection, causing large cyclic torques (peak-to-peak) which can cause mechanical vibration and damage to the shaft, couplings and the gearbox (if any). If the peak shaft stresses exceed the yield strength of the shaft material, then immediate cracks or breaks in the shaft may occur. Below this level, the length of time before cracking occurs is dependent upon the magnitude of the cyclic torques and the number of cycles, which occur each time the motor is disconnected and reconnected [10].

It is also important to look at the peak current experienced by the motors during residual voltage transfer. As detailed in Table I, the worst-case current (around 14 pu) occurred on Motor B with a closing angle of 205.47°. These high currents can cause both thermal as well as mechanical damage to stator conductors and their insulation. High currents can also cause tripping of motors due to the operation of motor instantaneous overcurrent protection relays and may cause tripping of the feeder and transformer overcurrent protection relays during residual voltage MBT.

B. Discussion of Comparison of Currents and Torques—Residual Voltage Transfer Versus Motor Start

As can be seen from Table I, in all of the cases, the peak currents and peak-to-peak torques observed during residual voltage transfer on all motors are greater than the motor start currents and torques respectively. In particular, in the majority of cases, the currents during transfer are well in excess of six times rated current, which is generally specified for across-the-line motor starting.

C. Discussion of Comparison of Currents and Torques—Residual Voltage Transfer Versus In-Phase Transfer

The in-phase transfer case reported here has to rotate through a significant angle to pass through zero degrees for a smooth synchronous close. The transfer takes more than 27 cycles, which is much more than the 10-cycle fast transfer window specified by ANSI C50.41. However, the bus voltage at the point of transfer is at 62% compared to 30% for a residual voltage transfer. The low bus voltage at 30% increases the probability that low voltage motor contactors may drop out during a residual voltage transfer. The frequency of the bus during the in-phase transfer reached 56.818 Hz and the corresponding pu V/Hz is 0.345 compared to worst-case residual voltage transfer where the frequency is 53 Hz and the corresponding V/Hz is 1.33 pu.

The transient torques experienced by the motors during an in-phase transfer are provided in Table I. The peak-to-peak torque in the case of in-phase transfer is less than one-half of the peak-to-peak torque during worst-case residual voltage transfer for all three motors (A, B, and C) simulated. The peak currents during in-phase transfer are lower than the motor start currents and, in all cases, lower than residual voltage transfer. This indicates that an in-phase transfer is a much better transfer method and can be successfully applied instead of a residual voltage transfer method when the fast transfer method is not a viable option due

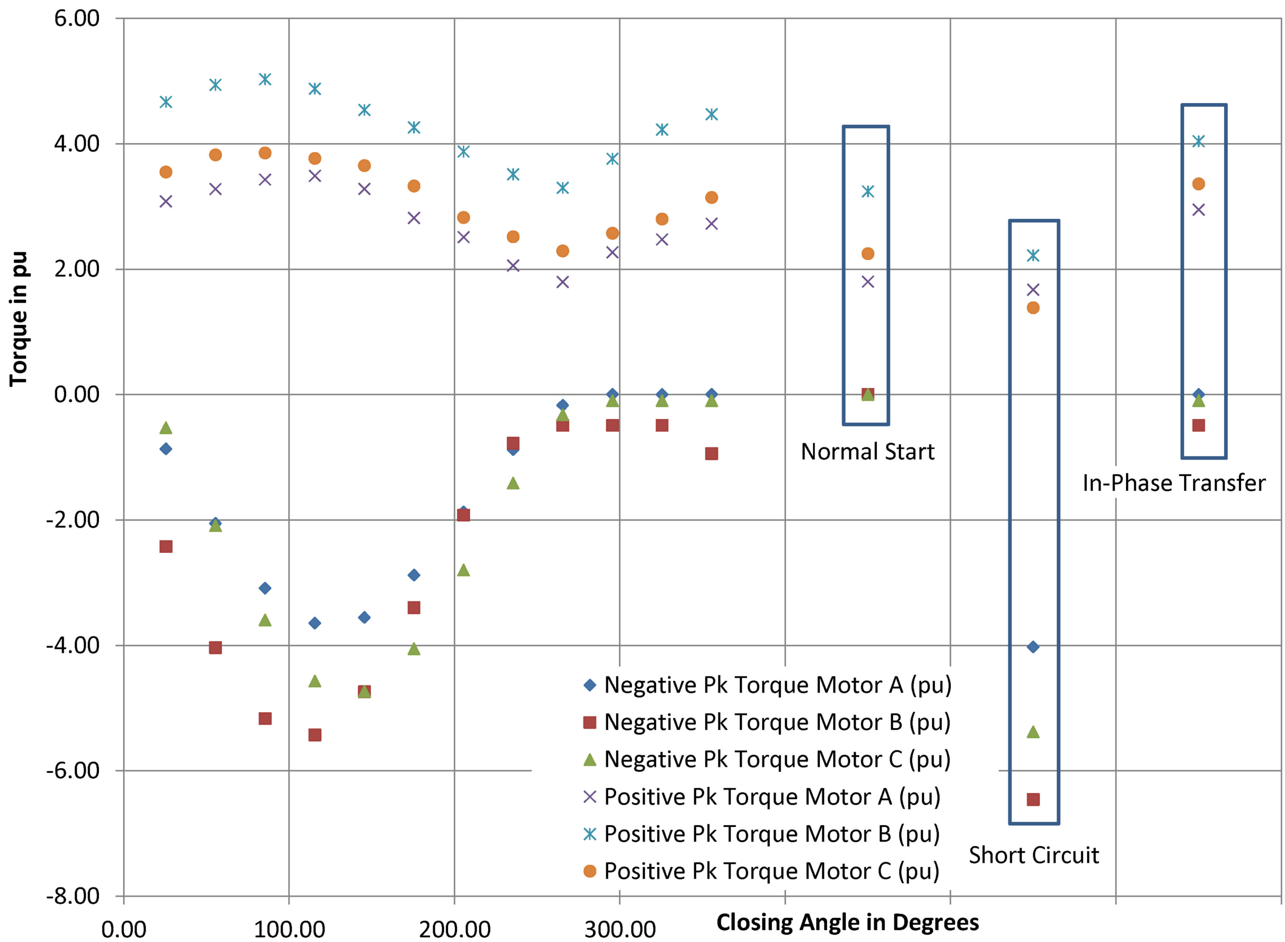

Fig. 11. Graph of positive and negative peak transient torque versus closing angle.

to a large initial angle between the motor bus and the backup source.

D. Discussion of Comparison of Currents and Torques—Residual Voltage Transfer Versus Motor Short Circuit

Referring to Table II, the peak-to-peak torque developed during the residual voltage transfer is higher than the severe SCT in 33% of the cases. For example, the worst-case peak-to-peak torque during residual voltage transfer for Motor A is 7.13 pu versus a SCT of 5.70 pu, for Motor B is 10.30 pu versus a SCT of 8.68 and for Motor C is 8.39 versus an SCT of 6.76. As the nature of these torques is cyclic or pulsating, this could generate high mechanical vibration resulting in possible cumulative damage to the motors and any mechanical equipment connected to them.

As described before, motors are usually designed to tolerate the currents and torques during short circuit on their terminals. This design criterion is based on the fact that the faults occur infrequently (fault-tolerant capability), not the normal operating criteria. As can be seen from Tables I and II, in 67% of the cases, motors are experiencing higher than short circuit currents during residual voltage transfers. High currents passing through the motor conductors cause high mechanical stresses on the conductors, fixed in stator slots by wedges, and held in end windings by a combination of epoxy, blocking, and lashings. This mechanical stress can result in damage to the insulation surrounding the stator conductors and, over time, it can cause a short circuit in the stator windings.

The graphs in Figs. 9–11 give a clear picture of the range of the currents and torques caused by residual voltage transfers, well in excess of those caused by a three-phase short circuit of all motors and many times a normal motor start or an in-phase transfer.

E. Best Curve Fit—Motor Transient Transfer Torque and Peak Current Versus Closing Angle

The peak current and transient peak-to-peak torque values in Table I and the corresponding graphs of the peak current and transient peak-to-peak torque for Motors A, B, and C against the twelve closing angles in Figs. 9 and 10 resemble a sinusoidal function with an offset.

A least squares (LS) curve fit technique is used to find the best curve fit for the transient peak-to-peak torque and the peak current with the following equations which represent a combination

TABLE II
RESIDUAL VOLTAGE TRANSFER VERSUS MOTOR SHORT CIRCUIT

Closing Angle	55.47	85.47	115.47	145.47	175.48	205.47	235.47	265.47	295.47	Short Circuit
Motor A Peak Current	**5.46**	**6.44**	**7.44**	**8.54**	**8.59**	**9.05**	**8.69**	**7.63**	**6.90**	**5.90**
Motor B Peak Current	**8.98**	**10.68**	**12.28**	**13.73**	**13.49**	**13.98**	**13.07**	**11.26**	**9.94**	**9.55**
Motor C Peak Current	**6.81**	**8.02**	**9.27**	**10.62**	**10.74**	**11.44**	**11.05**	**9.88**	**9.00**	**7.50**
Motor A Negative Peak Torque	-2.06	-3.09	-3.65	-3.56	-2.88	-1.88	-0.88	-0.17	0.00	**-4.03**
Motor B Negative Peak Torque	-4.04	-5.17	-5.43	-4.74	-3.40	-1.93	-0.78	-0.49	-0.49	**-6.46**
Motor C Negative Peak Torque	-2.09	-3.60	-4.57	-4.74	-4.06	-2.80	-1.41	-0.33	-0.10	**-5.38**
Motor A Positive Peak Torque	3.27	3.42	3.48	3.28	2.82	2.51	2.06	1.79	2.27	**1.67**
Motor B Positive Peak Torque	4.94	5.03	4.87	4.54	4.26	3.87	3.51	3.30	3.76	**2.21**
Motor C Positive Peak Torque	3.82	3.85	3.76	3.65	3.32	2.82	2.51	2.29	2.57	**1.38**
Motor A Transient Pk-to-Pk Torque	**5.33**	**6.52**	**7.13**	**6.83**	**5.70**	**4.39**	**2.94**	**1.97**	**2.27**	**5.70**
Motor B Transient Pk-to-Pk Torque	**8.98**	**10.20**	**10.30**	**9.28**	**7.66**	**5.80**	**4.29**	**3.79**	**4.25**	**8.68**
Motor C Transient Pk-to-Pk Torque	**5.91**	**7.45**	**8.34**	**8.39**	**7.38**	**5.62**	**3.93**	**2.61**	**2.67**	**6.76**

of a sinusoidal function along with a linearly varying offset as follows:

$$\mathrm{T_{P-P}}(\delta_\mathrm{k}) = (\mathrm{O_T} + \lambda_\mathrm{T}\, \delta_\mathrm{k}) + \mathrm{A_T}\, \sin(\delta_\mathrm{k} + \alpha_\mathrm{T}) \quad (20)$$

$$\mathrm{I_P}(\delta_\mathrm{k}) = (\mathrm{O_I} + \lambda_\mathrm{I}\, \delta_\mathrm{k}) + \mathrm{A_I}\, \sin(\delta_\mathrm{k} + \alpha_\mathrm{I}) \quad (21)$$

where $T_{P\text{-}P}$: Transient peak-to-peak torque in pu
I_P: Peak motor current in pu
δ_k: Closing angle at index k in radians
k: Index k (1 to 12) denotes k-th value of δ
O_T: Offset of the sinusoidal function for $T_{P\text{-}P}$ in pu
λ_T: Linear constant of the offset for $T_{P\text{-}P}$ in pu/radian
A_T: Amplitude of the sinusoidal function for $T_{P\text{-}P}$ in pu
α_T: Phase angle of the sinusoidal function for $T_{P\text{-}P}$ in radians
O_I: Offset of the sinusoidal function for I_P in pu
λ_I: Linear constant of the offset for I_P in pu/radian
A_I: Amplitude of the sinusoidal function for I_P in pu
α_I: Phase angle of the sinusoidal function for I_P in radians

TABLE III
LS CURVE FIT PARAMETERS

LS Curve fit parameter	Motor		
	A	B	C
O_T, pu	4.08	6.64	4.56
λ_T, pu/rad	0.0796	0.05	0.194
A_T, pu	2.7	3.35	3.36
α_T, degrees (radians)	-27.6 (-0.482)	-12.6 (-0.22)	-34.4 (-0.6)
O_I, pu	7.22	11.1	8.95
λ_I, pu/rad	-0.044	-0.082	-0.0135
A_I, pu	1.957	3.365	2.54
α_I, degrees (radians)	-107.4 (-1.87)	-95.1 (-1.659)	-110.3 (-1.92)

The LS curve fit, with a sinusoidal function plus linear offset using (20) and (21), yields the parameters shown in Table III. These parameters depend upon various factors including type of motor (compressor, pump, fan, etc.), motor impedances, inertia, and initial loading.

The delta voltage, the difference between the motor bus voltage and the new source voltage just prior to the residual voltage transfer breaker close, is related to the breaker closing angle. The RMS values of delta voltage and the square of the delta voltage are calculated for each of the breaker closing angles using a period of one half-cycle of the delta voltage just prior to closing. Fig. 12 shows the graphs of instantaneous and RMS values of delta voltage along with instantaneous values of motor bus voltage and new source voltage. For a given load, using (17) and (18), the stator current is proportional to the voltage applied to the stator, now altered by the delta voltage at close. The motor torque is proportional to the vector product of stator and rotor currents from (8) which in turn can be approximated to be proportional to the square of the applied stator voltage.

Assuming the magnitude of the motor bus voltage is constant at 0.3 pu and the new source voltage is 1.0 pu, the delta voltage varies approximately from 0.7 to 1.3 pu due to the decay of motor bus frequency and the resulting variation of angle between the motor bus voltage and new source voltage from 0° to 360°. The RMS value of the delta voltage can be represented by a sinusoidal function with an amplitude of 0.3 pu with an offset of 1.0 pu.

Figs. 13–15 show the graphs of positive peak torque, negative peak torque, and transient peak-to-peak torque, for Motors A, B, and C, respectively. In order to see the effect of negative peak torque on the LS curve fit values, the negative peak torque is inverted and plotted. These plots also show the LS curve fit, linearly varying offset, the sinusoidal function and the delta voltage square. The linear offset O_T is shown in the middle of these plots and the sinusoidal function is in the bottom of

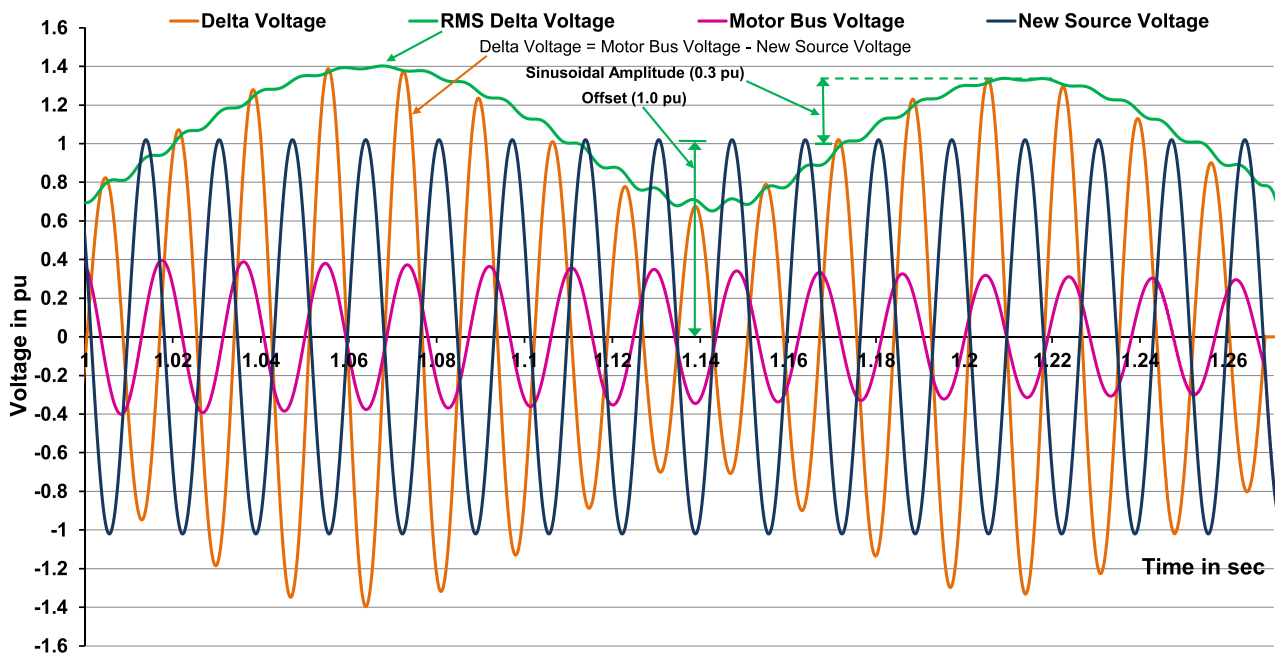

Fig. 12. Graph of instantaneous, RMS, and square of RMS value of delta voltage.

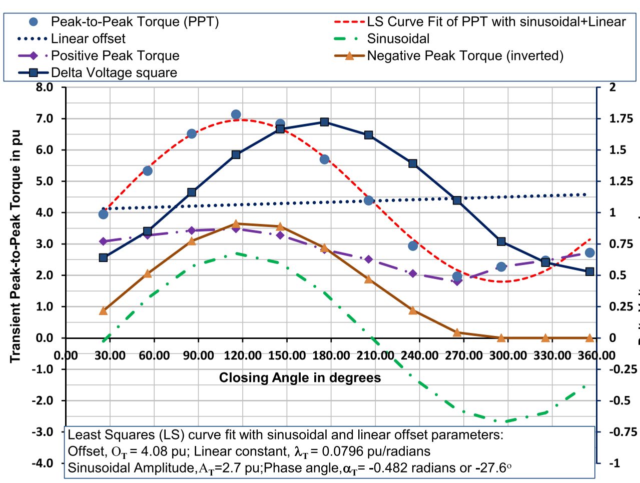

Fig. 13. Graph of Motor A transient peak-to-peak torque versus closing angle.

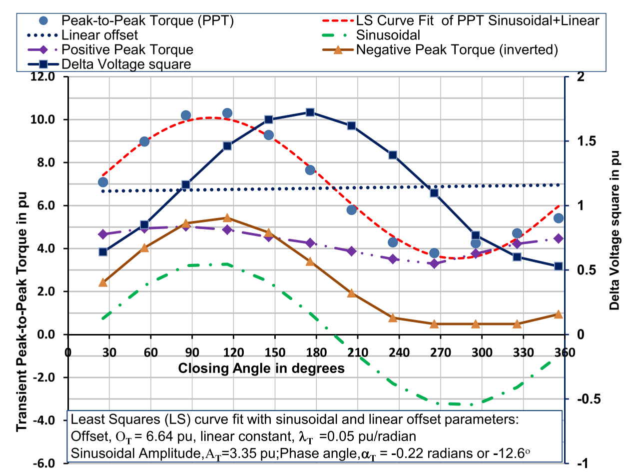

Fig. 14. Graph of Motor B transient peak-to-peak torque versus closing angle.

these plots. The sum of linearly varying offset and the sinusoidal function, denoted as LS Curve Fit of PPT, provides the best curve fit for the transient peak-to-peak torque by minimizing the sum of squares of the error between the data points of peak-to-peak torque and the LS curve fit plots.

The following observations can be made from these graphs. The variation of the peak positive torque versus closing angle is small; hence, the sinusoidal component of the transient peak-to-peak torque is mainly coming from the negative peak torque.

From the LS curve fit of transient peak-to-peak torque versus closing angle graphs, the sinusoidal function has a similar shape as the delta voltage square versus closing angle graphs shown in Figs. 13–15 and plotted on the alternate *Y*-axis. As discussed earlier, the torque can be approximated to be proportional to the square of the delta voltage. The offset O_T can be considered as a result of the offset of the sinusoidal function of RMS delta voltage squared. The amplitude of the sinusoidal variation of the peak-to-peak torque can be considered as a result of the amplitude of the sinusoidal variation of the delta voltage squared. Now from Figs. 13–15, the maximum value of the sinusoidal function is occurring at an angle of (90-α_T). This can be calculated as 117.6° for Motor A, 102.6° for Motor B, and 124.4° for Motor C. The linear offset constant λ_T is small for Motors A and B and can be ignored. For Motor C, λ_T needs to be included when using (20) to calculate transient peak-peak torque at different closing angles.

Figs. 16–18 show the graphs of peak motor current for Motors A, B, and C, respectively. These graphs also show the LS curve fit of peak current, the linearly varying offset, and the

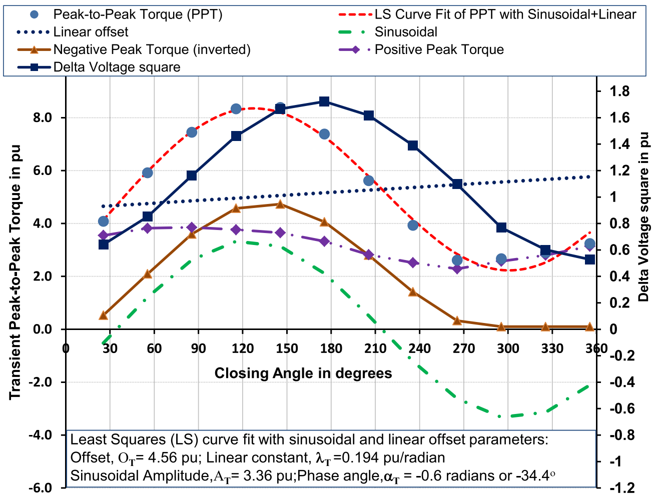

Fig. 15. Graph of Motor C transient peak-to-peak torque versus closing angle.

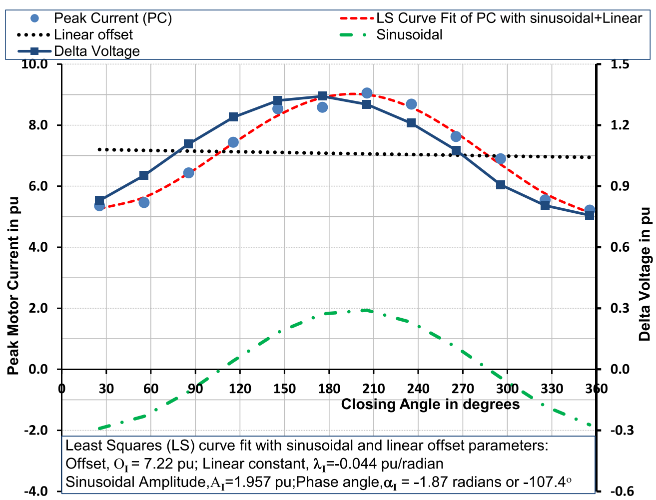

Fig. 16. Graph of Motor A peak current versus closing angle.

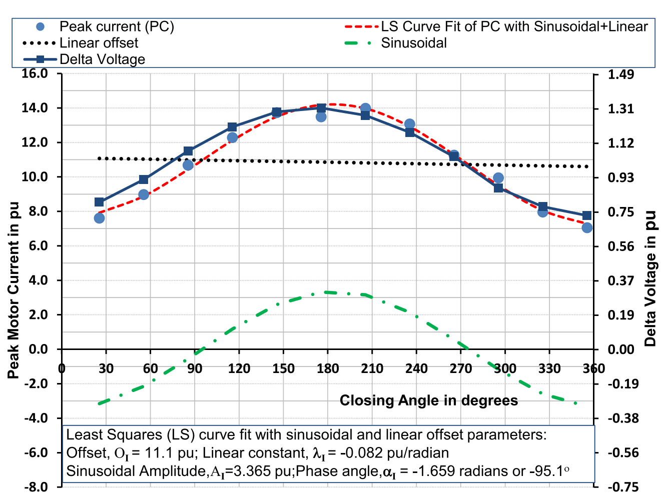

Fig. 17. Graph of Motor B peak current versus closing angle.

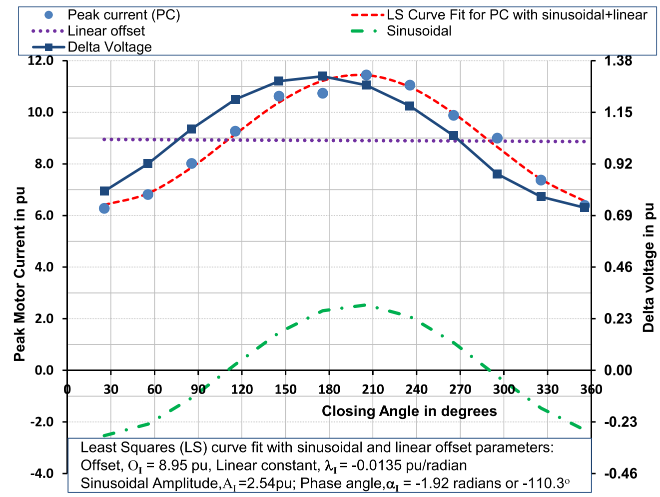

Fig. 18. Graph of Motor C peak current versus closing angle.

sinusoidal function. From the LS curve fit of peak motor current versus closing angle graphs, the sinusoidal function has a similar shape as the delta voltage versus closing angle graphs shown in Figs. 16–18 and plotted on the alternate *Y*-axis. As discussed earlier, the motor current is proportional to the RMS value of the delta voltage. The offset OI in (21) can be considered as a result of offset of a sinusoidal function of RMS delta voltage (see Fig. 12) and the amplitude of the sinusoidal variation of the peak current (A_I) can be considered as a result of the amplitude of the sinusoidal variation of the delta voltage.

In Figs. 16–18, the maximum value of the sinusoidal function is occurring at an angle of (90-α_I). The angle at maximum inrush current can be calculated as 197.4° for Motor A, 185.1° for Motor B, and 200.3° for Motor C. The linear offset constant λ_I for Motors A, B, and C in (21) are very small and can be ignored keeping the offset constant without causing any appreciable error.

For residual voltage transfers, the minimum peak inrush current occurs at a closing angle near 0° (or 360°) which coincides with the lowest delta voltage displayed in the graphs in Figs. 16–18. These peak inrush current magnitudes and delta voltages can be compared with those of the in-phase transfer method which is designed to assure a closing angle of 0°. As Table IV documents, the motor bus voltage during a residual voltage transfer is 0.3 pu, which results in a delta voltage of 0.7 pu, and the motor bus voltage during the in-phase transfer is 0.62 pu, which results in a delta voltage of 0.38 pu. Therefore, the delta voltage during a residual voltage transfer generating the minimum amount of peak inrush current is 84% higher than the delta voltage during an in-phase transfer with a 0° closing angle. Figs. 16–18 show a strong relationship between the peak inrush currents and the delta voltage, confirmed in Table IV where peak inrush currents during a residual voltage transfer are 52, 59, and 65 percent higher than those of an in-phase transfer. Therefore, the lower delta voltage during an in-phase transfer is the main factor in reducing the peak inrush currents even though the bus voltage

TABLE IV
RESIDUAL VOLTAGE VERSUS IN-PHASE TRANSFER

	Peak Inrush Currents (PC)		
Motor	In-Phase Transfer ΔV = .38pu @ Close	Residual Voltage Transfer ΔV = .7pu @ Close	Residual Voltage PC % > In-Phase
Motor A	3.44	5.22	52%
Motor B	4.44	7.05	59%
Motor C	3.88	6.39	65%

is much higher than the bus voltage during a residual voltage transfer. These results demonstrate that the in-phase transfer method is far superior to even the best 0° phase angle close by the residual voltage transfer method, which has only a 1 in 360 chance of ever occurring.

F. Discussion of Residual Voltage Transfer Results Related to Industry Standards

For years, ANSI/NEMA C50.41, Polyphase Induction Motors for Power Generating Stations, clauses 14.2 and 14.3 [11] have stipulated that the following.

1) A slow transfer can be performed if the closure of the alternate supply breaker "is delayed until the motor rotor flux linkages have decayed sufficiently so that the transient current and torque associated with the bus transfer or reclosing will remain within acceptable levels …" Specifically, it maintains that "Slow transfer or reclosing can be accomplished by a time delay relay equal to or greater than 1.5 times the open-circuit alternating-current time constant of the motor."
2) A fast transfer must occur "within a time period of 10 cycles or less."
3) All transfers can be completed at or below 1.33 per unit volts per Hz on the motor rated voltage and frequency basis.

The many simulation results with significantly out-of-phase residual voltage transfers clearly demonstrate that even below 30% voltage, the motors experience damaging multiples of rated torque. The ANSI/NEMA C50.41 advice that "Slow transfer or reclosing can be accomplished by a time delay relay equal to or greater than 1.5 times the open-circuit alternating-current time constant of the motor" is wrong. Torque is NOT within acceptable levels at large close angles, even at low voltage.

Clearly, the in-phase transfer in this study produced results well within the acceptable motor torque rating and yet the ANSI/NEMA C50.41 Standard of 10 cycles or less would reject this transfer. This study demonstrates that the "10 cycles or less" criteria must not be applied to the in-phase transfer method, as it may take more than 10 cycles for the motors to rotate back into synchronism and complete a synchronous transfer. Thus, the arbitrary 10-cycle limit must be ignored or risk blocking an otherwise perfectly good transfer. When an immediate fast transfer is not possible due to a large initial angle, the in-phase transfer allows the motors to rotate back into sync at the completion of the transfer. With the in-phase transfer method added as a synchronous method of "fast transfer" per the definition of C50.41, this 10-cycle restriction can be eliminated. Moreover, in the fast-moving world of MBT, 10 cycles (167 ms) is an eternity and never was a safe limit for the C50.41 fast transfer. Even at the medium inertia frequency decay of 20 Hz/s (R_S), with zero initial slip frequency (S_{INIT}), the angle movement ($\Delta Ø$) in 10 cycles (T), per the equation $\Delta Ø = 360(S_{INIT} + 0.5R_S T)T$, is a dangerous 100°. And this does not take into consideration that the initial phase angle may be nowhere near zero.

The pu V/Hz calculation depends on only three values at closure compared to the new source: the bus voltage difference, the bus frequency difference, and the phase angle difference. But since the pu V/Hz calculation ignores current, it cannot possibly address the torques that motors are experiencing. The results of the study confirm this as significantly out-of-phase residual voltage transfers with closures at damaging multiples of rated torque are all given passing grades equal or less than 1.33 pu V/Hz. Therefore, the use of the 1.33 pu V/Hz limit, and the fundamental metric itself must be eliminated as a criterion for the safe transfer of motor buses.

From the study results, residual voltage transfers have more than 33% probability of producing unacceptable high torque to motors greater than SCT, resulting in cumulative loss-of-life, motor fatigue, and potential early life failure. Residual voltage transfers provide the least opportunity for maintaining continuity of critical process motor loads, as the motors on the bus will have coasted down significantly in speed, possibly coupled with the jarring effect of a large phase angle at breaker closure which also affects shafts, couplings, and loads. This can subject the motors and loads to high inrush current and associated torque, lengthy undervoltage causing motor trip or dropout, and necessary load shed if the new source cannot reaccelerate all the motors simultaneously or if the transfer would cause excessive plant voltage dip.

Acknowledging these significant problems, some in the industry have elected to only perform dead transfers, waiting until the motors have stopped and then restarting the whole process. This strategy is extremely expensive and opens up exposure to the risk of having to perform an unnecessary complete shutdown and restart of the process. There is no need to resort to such extreme measures since synchronous fast and in-phase transfers always occur at much higher voltages, at much lower slip frequencies, and coupled with the synchronous closure, provide a far gentler transfer than the "blind" residual voltage method. Safe transfers can be performed rapidly and seamlessly with no effect on the process.

VII. CORROBORATING PRIOR WORK

In a 2017 IEEE PCIC paper [12], a new torque ratio criteria was developed to provide a measure that could be used to assess individual transfers. This MBT metric uses the voltage and current signals to calculate the power drawn by the motor and the corresponding torque ratio between the peak air gap torque after the transfer and the air gap torque, under steady-state load, prior to the transfer. The paper analyzed 36 live, online transfers, and graphed torque ratio versus Ø Angle at Close and observed a high correlation confirming one of the results of this study.

Furthermore, residual voltage transfer where the phase angle and slip frequency are ignored can produce dangerously high torques as significantly out-of-phase residual voltage transfers were recorded with torque ratios of 11.31 and 13.83, further confirming the results of this study.

This article confirmed with 32 live, online transfers that synchronous fast and in-phase transfers always occur at much lower torque ratios than the "blind" residual voltage transfer method.

References

[1] ANSI/NEMA C50.41-2012, Polyphase Induction Motors for Power Generating Stations, NEMA, Rosslyn, VA, p. 14, 2012.

[2] *IEEE Guide for AC Motor Protection*, IEEE Std. C37.96-2012, 2012.

[3] IEEE Std. C37.96-2012, Op Cit, p. 6, 2012.

[4] IEEE Std. C37.96-2012, Op Cit, p. 95, 2012.

[5] IEEE Std. C37.96-2012, Op Cit, p. 97, 2012.

[6] ANSI/NEMA C50.41-2012, Op Cit, p. 15, 2012.

[7] IEEE Std. C37.96-2012, Op Cit, pp. 95–97, 2012.

[8] P. C. Sen, *Principles of Electric Machines and Power Electronics*. Hoboken, NJ, USA: Wiley, 2007, ch 5.

[9] S. Ansuj, F. Shokooh, and R. Schinzinger, "Parameter estimation for induction machines based on sensitivity analysis," *IEEE Trans. Ind. Appl.*, vol. 25, no. 6, pp. 1035–1040, Nov./Dec. 1989.

[10] R. H. Daugherty, "Analysis of transient electrical torques and shaft torques in induction motors as a result of power supply disturbances," *IEEE Trans. Power App. Syst.*, vol. PAS-101, no. 8, pp. 2826–2836, Aug. 1982.

[11] ANSI/NEMA C50.41-2012, Op Cit, pp. 14–15.

[12] M. V. V. S. Yalla and T. R. Beckwith, "Expanded field data analysis in support of a torque-based motor bus transfer criterion," *IEEE Trans. Ind. Appl.*, vol. 54, no. 5, pp. 4983–4991, Sep./Oct. 2018, doi: 10.1109/TIA.2018.2834877.

[13] M. Yalla, A. Vakili, and T. Beckwith, "Calculation of transient torques on motors during a residual voltage motor bus transfer," presented at IEEE PCIC Conf., Cincinnati, OH, USA, Sep. 24–26, 2018.

Murty V.V.S. Yalla (Fellow, IEEE) received the BSEE degree from Jawaharlal Nehru Technological University, Kakinada, India, in 1981, the MSEE degree from the Indian Institute of Technology, Kanpur, India, in 1983, and the Ph.D. degree in electrical engineering from the University of New Brunswick, Fredericton, NB, Canada, in 1987.

He has been with Beckwith Electric Co. since 1989 and currently holds the position of President. He holds six U.S. patents in digital controls and protective relays. He is the Chair of the International Electrotechnical Commission (IEC, Geneva, Switzerland) Technical Committee 95, Measuring Relays and Protection Equipment. He was a U.S. delegate to the International Council on Large Electric Systems (CIGRÈ, Paris, France) for working groups on protecting and monitoring generating plants and power transformers. He was a member of the North American Electric Reliability Corporation (NERC) System Protection and Control Subcommittee.

Dr. Yalla is a 2006 IEEE Fellow for contributions in computer relays for power systems. He is currently the Vice Chair of the IEEE Power System Relaying and Control (PSRC) Committee of the Power and Energy Society. He is also a Member of the IEEE Industry Technical Support Leadership Committee (ITSLC) of PES acting as a liaison between IEEE PES and NERC. He was the former Chair of the Rotating Machinery Protection Subcommittee of IEEE PSRC Committee. He was working Group Chair of IEEE Standard C37.102-2006 "Guide for AC Generator Protection;" IEEE PES tutorial Co-Author "Protection of Synchronous Generators;" and received the 2004 IEEE PES Working Group Recognition Award for outstanding technical report. He was the recipient of the IEEE Florida Council Outstanding Engineer Award in 2005, and the IEC 1906 Award in 2010, which honors IEC experts worldwide.

Arman Vakili (Senior Member, IEEE) received the BSEE degree from Tehran Azad University, Tehran, Iran, in 1999.

He has more than 17 years of experience in the electric power industry, encompassing the fields of design of power system protection, field applications and commissioning. He has served as Field Engineering Manager for APD in Perth, Australia, Senior Consultant for AECOM and as Technical Manager of BBA. Beginning in 2000, he worked for substation commissioning groups in Iran, commissioning several 400 kV substations, including protection systems. He also worked on the modeling of protection systems. He was Lead Electrical Engineer with Powell Industries and is currently with Malayer Engineering Services.

Vakili is a member of the Power Engineering Society and the Industry Applications Society and has served on various working groups in the Power Systems Relaying Committee.

Thomas R. Beckwith (Life Member, IEEE) received the BSEE degree from Case Western Reserve University, Cleveland, OH, USA, in 1969, and the MBA degree from the University of South Florida, Tampa, FL, USA, in 1990.

He is a Co-Inventor of a 1993 U.S. patent on a Multifunction Protective Relay System. Currently the CEO of Beckwith Electric Co., he previously held positions as Production Manager, Vice President of Sales and Marketing, and President of Beckwith Engineering Services and Training. Since 1970, he has served as R&D Design Engineer, Systems Engineer and Field Commissioning Engineer.

Beckwith is a Life Member of the IEEE PES and IAS and has served on working groups in the Power System Relaying Committee since 1972. He was the Chair of the working group IEEE C37.90.1-2012 Standard for Surge Withstand Capability Tests for Relays and Relay Systems Associated with Electric Power Apparatus.